

The Mathematical Calculations on Absorbance-wavelength Relation of Zinc, Cobalt and Indium Peripherally /Non-Peripherally Metallo Phthalocyanines Bearing Zingerone Moieties

Bülent Kıyak^a, Emre Eroğlu^{b*} and Aliye Aslı Esenpınar^{c*}

^a Marmara University, Faculty of Art and Science, Department of Chemistry, Kadıkoy 34722, Istanbul, Turkey

^b Kırklareli University, Department of Mathematics, 39100, Kırklareli, Turkey

^c Kırklareli University, Department of Chemistry, 39100, Kırklareli, Turkey

Corresponding Author: [Aliye Aslı Esenpınar](mailto:Aliye.Asli.Esenpinar@kkl.edu.tr)

ABSTRACT: The zinc, cobalt and indium phthalocyanines carrying four vanillylacetone or zingerone in the peripherally and non-peripherally have prepared by cyclotetramerization of 4-[2-methoxy-4-(3-oxobutyl) phenoxy] phthalonitrile / 3-[2-methoxy-4-(3-oxobutyl) phenoxy] phthalonitrile have been investigated mathematical modeling properties.

The novel chromogenic compounds characterizing (A-F) variables are given with linear and nonlinear models in the mathematical aspect.

KEYWORDS. :Phthalocyanine; Vanillylacetone; Zingerone; Mathematical Modeling.

Date of Submission: 15-02-2019

Date of acceptance: 28-02-2019

I. INTRODUCTION

Vanillylacetone (Zingerone) is a phenolic alkanone. It is isolated from the root of the ginger, also a flavor component of the mustard oil, mango, cranberry and raspberry. In ginger, it is formed by the retro-aldol reaction from its natural precursor, gingerol by cooking [2]. Zingerone is used to treat a variety of medical applications. Zingerone's derivatives have been done showing that a topically applied extract containing it may help prevent some skin cancers. Zingerone also has a major role in lipid oxidation since it is an anti-oxidant [3].

Since nature has provided many effective anticancer agents, plant-derived drug research has been made significant progress in anticancer therapies [4-7].

Phthalocyanine (Pc) is a tetramer macrocycle which is a planar conjugated array of 18- π electrons exhibiting aromatic behavior, formed from four isoindolines linked via azo-bridge [8]. Pcs have widely used as blue and green light-resistant pigments and dyes in the paper and textile industries because of their high thermal, chemical, and photochemical stabilities [9]. A lot of application has been devoted to the possible use of metallophthalocyanines (MPcs) as a functional substance in solar cells [7], as a detecting component in chemical sensors [7,8], in optical storage medium [7-9], as a photoconducting agent in photocopying machines [7-10], as an electrocatalyst [7-11]. In addition, Pcs have found application area in photodynamic therapy (PDT). Because of the lack of selectivity towards tumor cells and the lack of isomeric purity, the present drugs used presently for PDT have certain limitations [12-14]. This type of therapy combines light, oxygen and a photosensitizing drug to cause specific cell damage [15]. For example the PDT properties of the phthalocyanine dyes are strongly influenced by the presence and nature of the central metal ion and substituents. Also, the presence of electron-donating/electron-withdrawing substituents is a useful way of regulating the wavelength of the Q band to longer or short wavelengths [16-18].

For the concentrating a more mathematical perspective, one should discuss the relationships between elements and wavelength (λ), separately. This work rigidly obeys to chemical principles and includes math-based different discussions. This obedience via cause-effect relationship and causality principle [19, 20] governs Zn, Co, In and wavelength (λ) correlations. In this study, we focus on the variables of the experiment of peripherally / non-peripherally metallo phthalocyanines (**Scheme**) and we discuss mathematical models relating

to the event. As in the former studies [21, 22], the models are visualized and the reader is given the opportunity to compare correlation data. Although binary linear models have difficulty in the elucidating exact relationship between variables, the presentation of these models is essential. Weak correlation encourages scientists to search for nonlinear models. Mathematical models offer information to researchers about data and their relationships, even if they are in different areas. In addition, they should give clues about the actions of the variables under different conditions [20, 23]. The ultimate aim of the study is to reach the essential results of the experiment by the mathematical modeling without into the laboratory. For the first time in this discussion, it is tried to save time and labor by modeling the interaction of metals used in cancer studies. The authors analyze the significant correlation between variables and then establish a template.

II. MATHEMATICAL MODELING

The relevant variables of the experiment are listed in Table 2. Table 3 indicates the correlation between all data. Values close to one in the correlation matrix indicate a high relationship level. Variables that are strongly related with each other are expected to be mutually effective in the experimental process.

Table 2. Descriptive analysis

	N	Minimum	Maximum	Mean	Std. Deviation	Variance
$\lambda(\text{nm})$	501	300	800	550.00	150.544	20958.500
A	501	.007	.224	.04401	.050282	.003
B	501	.007	.328	.07651	.082397	.007
C	501	.010	.399	.07816	.075675	.006
D	501	.009	.967	.14416	.195389	.038
E	501	.008	.117	.03825	.029804	.001
F	501	.008	.127	.031829	.031829	.001

Table 3. Pearson's correlation matrix for the experiment variables

	$\lambda(\text{nm})$	A	B	C	D	E	F
$\lambda(\text{nm})$	1	-.433**	-.294**	-.237**	-.224**	-.484**	-.408**
A		1	.736**	.590**	.879**	.581**	.781**
B			1	.943**	.671**	.681**	.988**
C				1	.540**	.624**	.919**
D					1	.356**	.688**
E						1	.714**
F							1

**Correlation are significant at the 0.01 level (2-tailed)

One can decide whether the data are suitable for normal distribution by using the KMO and Bartlett's Test in Table 4. This test demonstrates the suitability of the variables for factor analysis. When the consistency, sufficiency and normal distribution of the data are considered, the test value is expected to close to 1.

Table 4. KMO and Bartlett's Test

Kaiser-Meyer-Olkin Measure of Sampling Adequacy.		.742
Approx. Chi-Square		5427.584
Bartlett's Test of Sphericity	df	21
	Sig.	.000

Variables cluster is displayed in Figure 2 hierarchically. The figure is dendrogram of two main phases. The first phase 1,(4),8,(11),15,(18),22,(25)-tetrakis[2-methoxy-4-(3-oxobutyl)phenoxy]phthalocyaninato zinc (A), 1,(4),8,(11),15,(18),22,(25)-tetrakis[2-methoxy-4-(3-oxobutyl)phenoxy]phthalocyaninato cobalt (B), 1,(4),8,(11),15,(18),22,(25)-tetrakis[2-methoxy-4-(3-oxobutyl)phenoxy] phthalocyaninato indium (C), 2(3), 9(10), 16(17), 23(24)-Tetrakis [2-methoxy-4-(3-oxobutyl)phenoxy]phthalocyaninato zinc (D), 2(3), 9(10), 16(17), 23(24)-Tetrakis[2-methoxy-4-(3-oxobutyl)phenoxy] phthalocyaninato cobalt (E), 2(3), 9(10), 16(17), 23(24)-Tetrakis[2-methoxy-4-(3-oxobutyl)phenoxy]phthalocyaninato indium (F) and the second phase is λ which are beneficial substances.

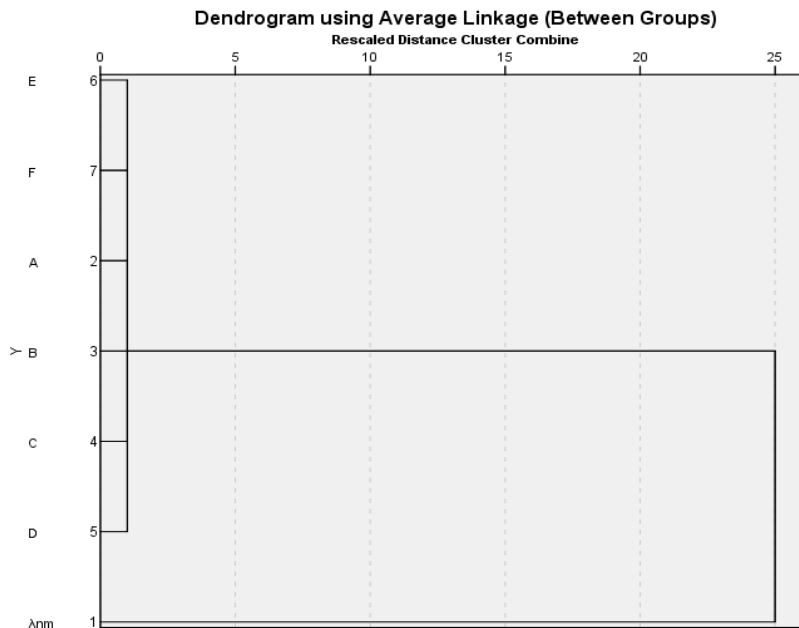


Figure 2. Dendrogram of hierarchical cluster analysis.

The seven variables found in the data simplification method are capable of explaining the event via the two maximum eigenvalues with 82.1%. This ratio, as shown in Table 5, is obtained by using Kaiser Normalization of the rotation for Principal Component Analysis extraction and Varimax method.

Table 5. Total variance explained

Component	Initial Eigenvalues			Extraction Sums of Squared Loadings		
	Total	% of Variance	Cumulative %	Total	% of Variance	Cumulative %
1	4.792	68.455	68.455	4.792	68.455	68.455
2	1.001	13.676	82.132	1.001	82.132	82.132

Scattering plot of these variables is shown in Figure 3. It is ranked from the maximum between the variables, with the showing a factor between every two points.

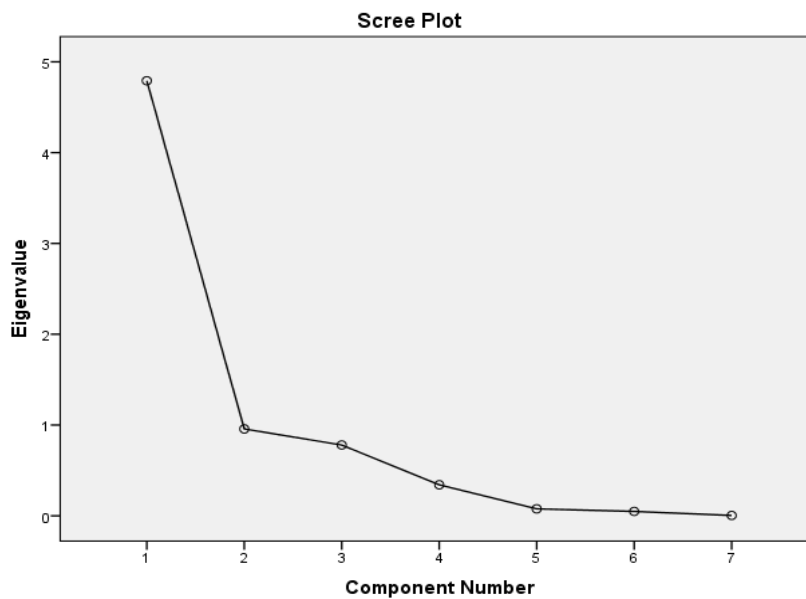


Figure 3. Scree plot for eigenvalues

The first two-main axes give details 82.1% of total variance. Meanwhile rotated component matrices of this factor weights are presented in Table 6.

Table 6. Rotated component matrix

Component	$\lambda(\text{nm})$	A	B	C	D	E	F
1	-.570	.897	.960	.848	.793	.823	.981
2	.324	.804	.922	.719	.629	.678	.962

From **Table 6**, two basic linear weight models can be written.

$$\text{Axes 1} = -(0.570)\lambda + (0.897)A + (0.960)B + (0.848)C + (0.793)D + (0.823)E + (0.981)F$$

$$\text{Axes 2} = (0.324)\lambda + (0.804)A + (0.922)B + (0.719)C + (0.629)D + (0.678)E + (0.962)F$$

2.1. Linear and nonlinear model

The regression model is:

$$y_i = f_i(x, b) + \varepsilon_i = \sum_{j=1}^n b_j x_j + \varepsilon_i$$

where y_i is dependent variable, x_j n-dimensional independent variable and ε_i is error. $f_i(x, b)$ called the expectation function for the regression model.

The sample covariance s_{jk}^2 is:

$$s_{jk}^2 \equiv \frac{\frac{1}{n-1} \sum_{i=1}^n \left[\frac{1}{\sigma_i^2} (x_{ij} - \bar{x}_j)(x_{ik} - \bar{x}_k) \right]}{\frac{1}{n} \sum_{i=1}^n \left(\frac{1}{\sigma_i^2} \right)}$$

where $j, k = 1, 2$; σ_i^2 is the standard deviation, n is the number of data points and \bar{x}_j is

$$\bar{x}_j \equiv \frac{\sum_{i=1}^n \left(\frac{x_{ij}}{\sigma_i^2} \right)}{\sum_{i=1}^n \left(\frac{1}{\sigma_i^2} \right)}$$

The sample variance is given by $s_j^2 \equiv s_{jj}^2$. The correlation coefficient can be expressed in terms of $r_{jk} \equiv \frac{s_{jk}^2}{s_j s_k}$.

Square of multiple-correlation coefficient R^2 is:

$$R^2 \equiv \sum_{j=1}^n \left(b_j \frac{s_{jy}^2}{s_y^2} \right) = \sum_{j=1}^n \left(b_j \frac{s_j}{s_y} r_{jy} \right)$$

R^2 is the percentage of the event definition of the model. The closer to R^2 is to one (1) in the established model, the greater the percentage of the model's description of the event is (Freund, 1979).

2.2. Relationship among variables

The variables discussed above as a whole, are investigated separately in this section with their three-linked and four-linked forms. In **Table 7**, the values in the left column belong to 4-linked variables and the values in the right column belong to 3-linked variables.

Table 7. KMO and Bartlett's Test

Kaiser-Meyer-Olkin Measure of Sampling Adequacy.		.571	.655
Bartlett's Test of Sphericity	Approx. Chi-Square	1705.300	1117.854
	df	6	6
	Sig.	.000	.000

As can be seen from KMO and Bartlett's Test, 3-linked variables have stronger relationships than 4-linked variables. It can be said that the factors of this association are more suitable than the normal distribution 3-linked ones. Dendrogram of hierarchical cluster analysis of 4-linked and 3-linked elements are shown in **Figure 4**, respectively.

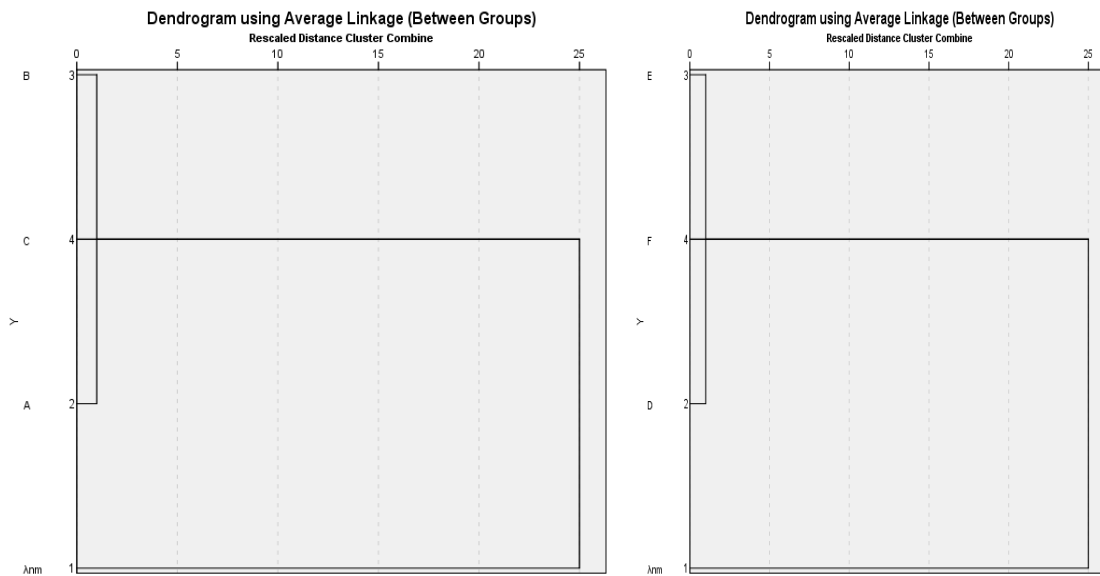


Figure 4. Dendrogram of hierarchical cluster analysis

Scattering plot of experiment variables is presented in **Figure 5**. It shown between two points as a factor gives clues about variables.

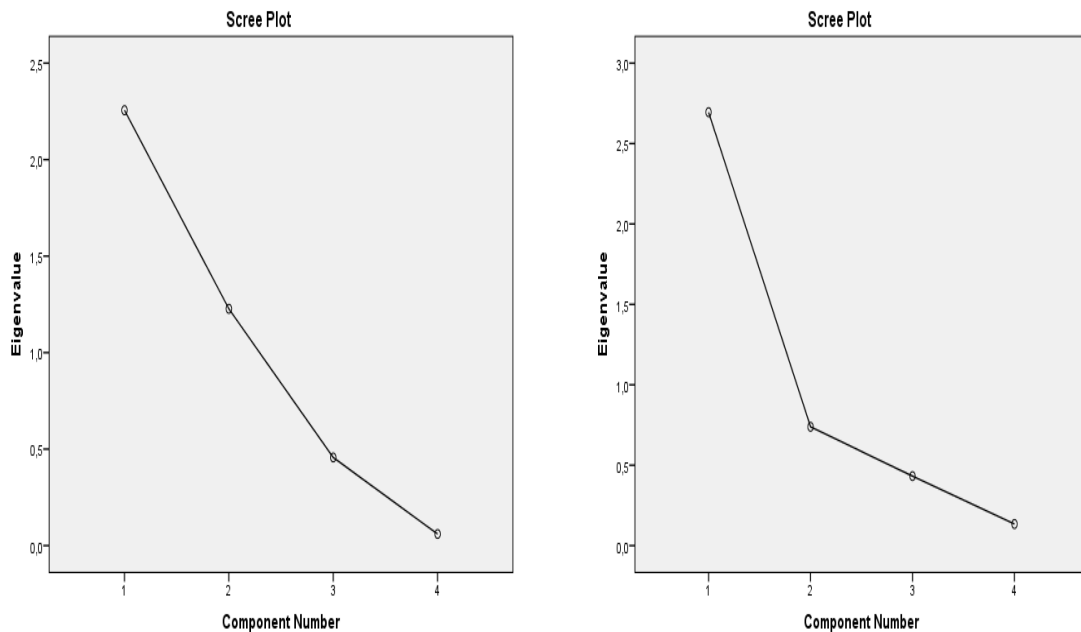


Figure 5. Scree plot for eigenvalues

On the left side of **Table 8**, there is a heap of 4-linked variables while on the right side a heap of 3-linked variables is located.

Table 8. Component matrix

Component	λ (nm)	A	B	C	λ (nm)	D	E	F
1	-.606	.876	.960	.868	-.701	.764	.864	.934

From **Table 8**, two basic linear weight models can be written.

$$\text{Axes 1} = -(0.606)\lambda + (0.876)A + (0.960)B + (0.868)C$$

$$\text{Axes 2} = -(0.701)\lambda + (0.764)D + (0.864)E + (0.934)F$$

In **Table 9**, it is seen that 4-linked variables have the ability to be able to explain the event with two factors and 87% while 3-connected variables have the ability to be able to explain the event 67.3% with only one factor.

Table 9. Total variance explained

Component	Initial Eigenvalues		% of Variance			Cumulative %	
	Total						
1	2.256	2.695	56.402	67.373	56.402	67.373	
2	1.227	.739	30.678	18.468	87.081	85.841	

Table 10 presents the variance analysis of A and D. Regression coefficients in the analysis are significant. This table refers to the described model and the residues. On the left side of **Table 10** and **11**, there is 4-linked variables while on the right side 3-linked variables is located. **Table 11** shows the model of A and D as:

$$A = (2.494) - (0.014)\lambda + (2.392 \times 10^{-5})\lambda^2 - (1.372 \times 10^{-8})\lambda^3,$$

$$D = (5.920) - (0.033)\lambda + (5.942 \times 10^{-5})\lambda^2 - (3.480 \times 10^{-8})\lambda^3$$

where multiple determination coefficient R is 0.904 and 0.628, respectively.

Table 10. Anova (Analysis of variance)

Model	Sum of Squares	df	Mean Square	F	Sig.	Sum of Squares	df	Mean Square	F	Sig.
Regression	1.965	3	.655	773.193	.000	8.603	3	2.868	112.235	.000
Residual	.438	517	.001			13.210	517	.026		
Total	2.402	520				21.813	520			

Table 11. Regression coefficients

Model	Unstandardized Coefficients		Standardized Coefficients		Sig.	Unstandardized Coefficients		Standardized Coefficients		Sig.
	B	Std. Error	Beta	t		B	Std. Error	Beta	t	
	(Constant)	2.494	.067			37.237	.000	5.920	.368	
λ (nm)	-.014	.000	-.29918	-33.453	.000	-.033	.002	-.24061	-14.760	.000
λ^2 (nm)	2.392×10^{-5}	.000	57.663	30.850	.000	5.942×10^{-5}	.000	47.531	13.950	.000
λ^3 (nm)	-1.372×10^{-8}	.000	-28.607	-31.751	.000	-3.480×10^{-8}	.000	-24.075	-28.230	.000

Figure 6 shows the nonlinear relationship between A and D with Lambda Wavelength. Note that the peak around the wavelength of 700 nm led to a declination in the nonlinear model of the D and downed the multiple determination coefficient.

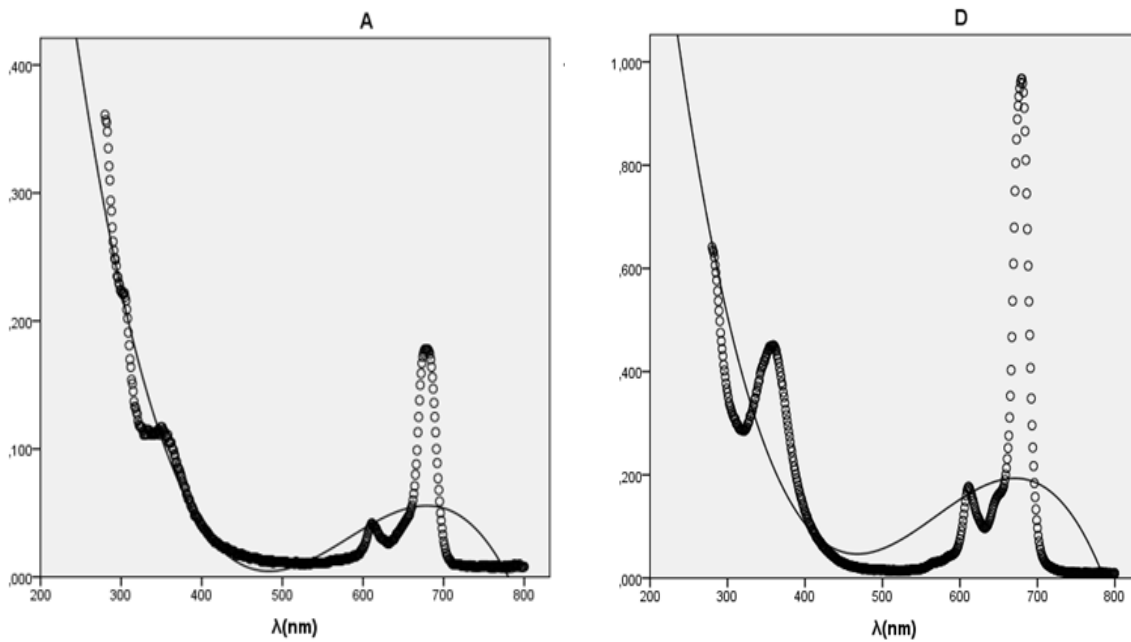


Figure 6. Nonlinear relationship between A, D and Wavelength λ(nm).

Table 12 presents the variance analysis of B and E. Regression coefficients in the analysis are significant. This table refers to the described model and the residues. On the left side of Table 12 and 13, there is 4-linked variables while on the right side 3-linked variables is located. Table 13 shows the model of B and E as:

$$B = (3.032) - (0.016)\lambda + (2.901 \times 10^{-5})\lambda^2 - (1.661 \times 10^{-8})\lambda^3,$$

$$E = (0.904) - (0.005)\lambda + (7.619 \times 10^{-6})\lambda^2 - (4.170 \times 10^{-9})\lambda^3$$

where multiple determination coefficient R is 0.780 and 0.843, respectively.

Table 12. Anova (Analysis of variance)

Model	Sum Squares	of df	Mean Square	F	Sig.	Sum Squares	of df	Mean Square	F	Sig.
Regression	2.671	3	.890	267.824	.000	.396	3	.132	424.911	.000
Residual	1.718	517	.003			.161	517	.000		
Total	4.389	520				.556	520			

Table 13. Regression coefficients

Model	Unstandardized Coefficients		Standardized Coefficient	Sig.	Unstandardized Coefficients		Standardized Coefficient	Sig.
	B	Std. Error			B	Std. Error		
(Constant)	3.032	.001		.000	.904	.041		.000
λ(nm)	-.016	.000	-.26821	.000	-.005	.000	-.20855	.000
λ ² (nm)	2.901x10 ⁻⁵	.000	51.735	.000	7.619 x10 ⁻⁶	.000	38.161	.000
λ ³ (nm)	-1.661x10 ⁻⁸	.133	-25.618	.000	-4.170x10 ⁻⁹	.000	-18.064	.000

Figure 7 indicates the nonlinear relationship between B and E with Lambda Wavelength. Note that the peak around the wavelength of 700 nm led to a declination in the nonlinear model of the B and downed the multiple determination coefficient.

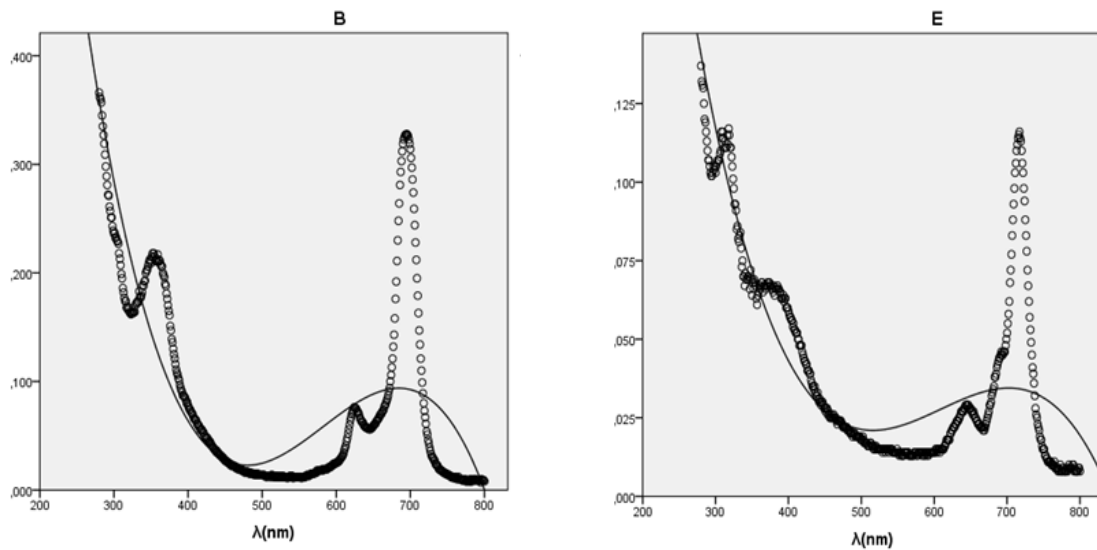


Figure 7. Nonlinear relationship between B, E and Wavelength λ(nm).

Table 14 presents the variance analysis of C and F. Regression coefficients in the analysis are significant. This table refers to the described model and the residues. On the left side of Table 14 and 15, there is 4-linked variables while on the right side 3-linked variables is located. Table 15 shows the model of C and F as:

$$C = (2.010) - (0.011)\lambda + (1.940 \times 10^{-5})\lambda^2 - (1.123 \times 10^{-8})\lambda^3,$$

$$F = (1.237) - (0.007)\lambda + (1.150 \times 10^{-5})\lambda^2 - (6.541 \times 10^{-9})\lambda^3$$

where multiple determination coefficient R is 0.587 and 0.840, respectively.

Table 14. Anova (Analysis of variance)

Model	Sum of Squares	df	Mean Square	F	Sig.	Sum of Squares	df	Mean Square	F	Sig.
Regression	1.048	3	.349	90.737	.000	.516	3	.172	413.414	.000
Residual	1.991	517	.004			.215	517	.000		
Total	3.040	520				.731	520			

Table 15. Regression coefficients

Model	Unstandardized Coefficients		Standardized Coefficients		t	Sig.	Unstandardized Coefficients		Standardized Coefficients		t	Sig.
	B	Std. Error	Beta				B	Std. Error	Beta			
(Constant)	2.010	.143			14.072	.000	1.237	.047			26.340	.000
λ(nm)	-.011	.001	-.21.315		-12.571	.000	-.007	.000	-.26.307		-23.152	.000
λ ² (nm)	1.940x10 ⁻⁵	.000	41.581		11.734	.000	1.150 x10 ⁻⁵	.000	50.229		21.151	.000
λ ³ (nm)	-1.123x10 ⁻⁸	.000	-20.812		-25.001	.000	-6.541x10 ⁻⁹	.000	-24.715		-35.142	.000

Figure 8 displays the nonlinear relationship between C and F with Lambda Wavelength. Note that the peak around the wavelength of 700nm led to a declination in the nonlinear model of the In4 and downed the multiple determination coefficient.

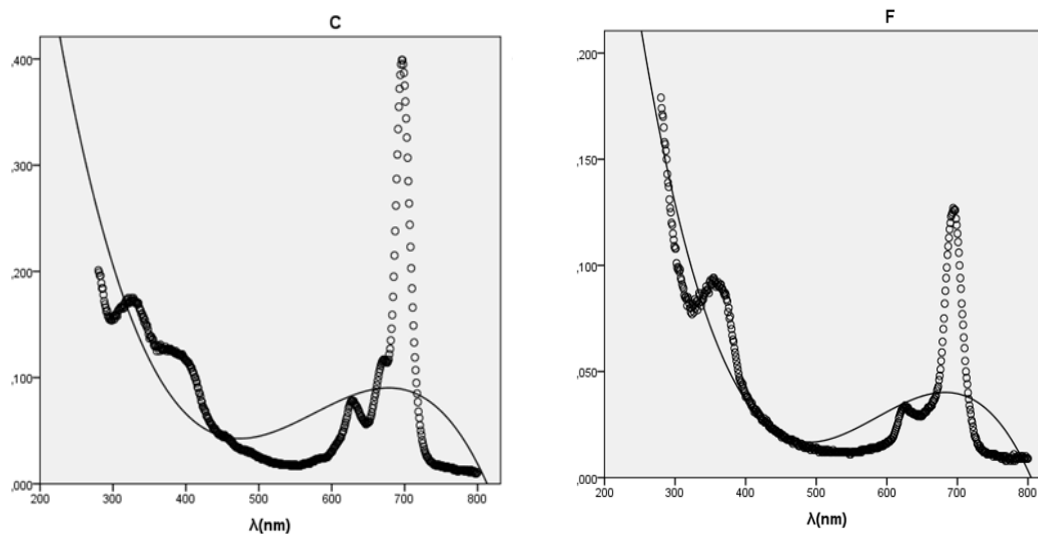
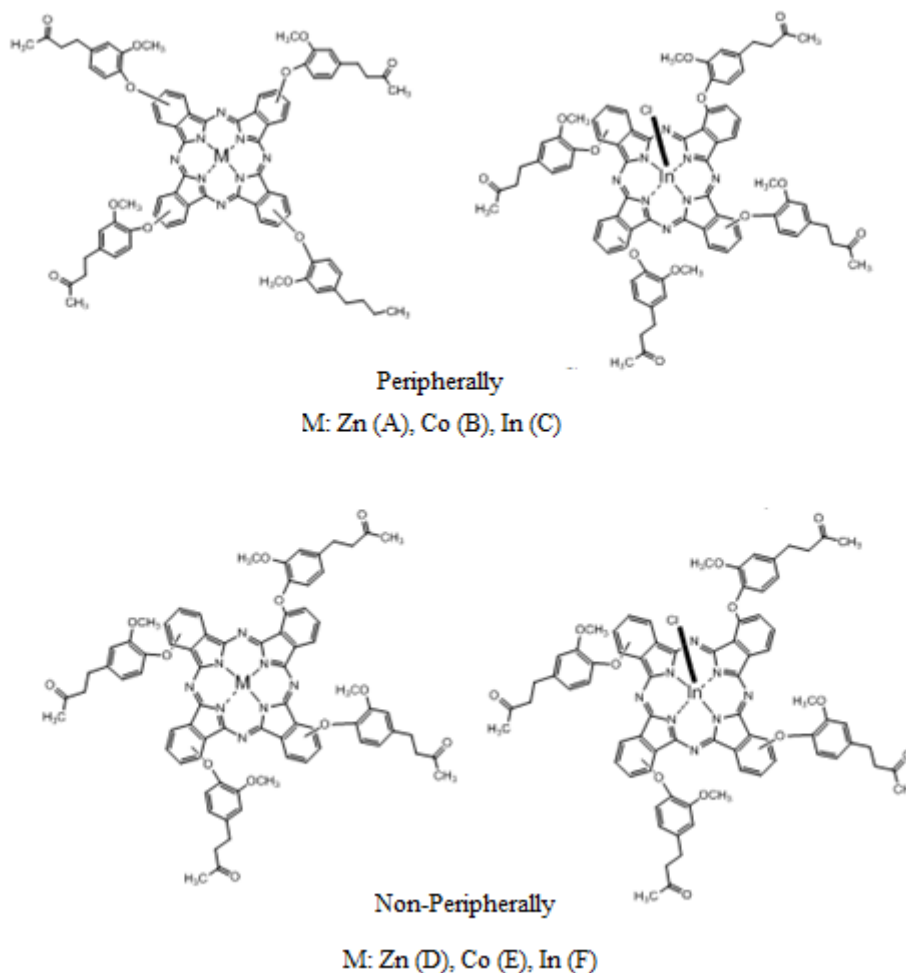


Figure 8. Nonlinear relationship between C, F and Wavelength λ (nm).



Scheme: The peripherally and non-peripherally metallo phthalocyanines.

III. CONCLUSION

This study has focused on the Zinc, Cobalt and Indium Peripherally /Non-Peripherally Metallo Phthalocyanines Bearing Zingerone Moieties, such an important experiment is viewed as a whole in order to be able to investigate it with all the details, just as it was in the Synthesis characterization photophysical and photochemical properties of zinc and indium phthalocyanines bearing a vanillylacetone moiety known as an anticarcinogenic agent. In the event, elements and wavelength indices are discussed and the cause-effect relationship is obeyed. All possible binary or multiple relationship and models are presented to the reader even if not statistically significant. Every model that produced about the experiment has been meticulously analyzed. The nonlinear model among variables is discussed for the first time by the authors. All results are in the 95% confidence interval. Graphs and tables have visualized the correlation among variables, as well as their interactions with each other.

The aim of in this study is to analyze the mathematical relationship between wavelength and other variables, and also to investigate the anticancer effects of phthaocyanines when the relationship between all variables is examined.

ACKNOWLEDGEMENTS

This work was supported by Kırklareli University (Project number: KLÜ-BAP-040 and KLÜ-BAP-043).

REFERENCES

- [1]. B. Kıyak, A. A. Esenpınar Kıyak, M. Bulut, Synthesis characterization photophysical and photochemical properties of zinc and indium phthalocyanines bearing a vanillylacetone moiety known as an anticarcinogenic agent. *Polyhedron*, 90 (2015) 183-196. <https://doi.org/10.1016/j.poly.2015.01.043>.
- [2]. D. Banji, O.J.F. Banji, B. Pavani, K. Ch. Kumar, A.R. Annamalai, Zingerone regulates intestinal transit, attenuates behavioral and oxidative perturbations in irritable bowel disorder in rats. *Phytomedicine*. 21 (2014) 423-429. <https://doi.org/10.1016/j.phymed.2013.10.007>.
- [3]. S.G. Shin, J.I.Y. Kim, H.Y. Chung, J.I.C. Jeong, *J. Agric. Food Chem.* 53 (19) (2005) 7617-7622. <https://doi.org/10.1021/jf051014x>.
- [4]. H.T. Lawless, D.A. Stevens, Responses by humans to oral chemical irritants as a function of the locus of stimulation. *Percept. Psychophys.* 43 (1988) 72-78.
- [5]. F. Borrelli, R. Capasso, A. Pinto A.A. Izzo, Inhibitory effect of ginger (*Zingiber officinale*) on rat ileal motility in vitro. *Life Sci.* 74 (2004) 2889-2896. <https://doi.org/10.1016/j.lfs.2003.10.023>.
- [6]. J. Gruenwald, T. Brendler, C. Jaenicke, PDR for herbal medical economics company; Montvale: New Jersey, 2000.
- [7]. H. J. Eichhorn, Mesomorphic phthalocyanines, tetraazaporphyrins, porphyrins and triphenylenes as charge-transporting materials. *J. Porphyr. Phthalocya.* 4 (2000) 88-102. [https://doi.org/10.1002/\(SICI\)1099-1409\(200001/02\)4:1<88::AID-JPP208>3.0.CO;2-6](https://doi.org/10.1002/(SICI)1099-1409(200001/02)4:1<88::AID-JPP208>3.0.CO;2-6).
- [8]. C.C. Leznoff Lever ABP. *Phthalocyanines: Properties and Applications*; VCH: New York, NY, USA, 1993.
- [9]. M. Hanack M. Lang, *Conducting Stacked Metallophthalocyanines and Related Compounds*. *Adv. Mater.* 1994 6 819-833. <https://doi.org/10.1002/adma.19940061103>.
- [10]. C.S. Frampton, J.M. O'Conner, J.I.M. Peterson, J. Silver, *Displays* 9 (4) 1988 174-178. [https://doi.org/10.1016/0141-9382\(88\)90064-9](https://doi.org/10.1016/0141-9382(88)90064-9).
- [11]. J.H. Zagal, Enhanced colours and properties in the electrochromic behaviour of mixed rare-earth-element bisphthalocyanines. *Coord. Chem. Rev.* 119 (1992) 89-136. [https://doi.org/10.1016/0010-8545\(92\)80031-L](https://doi.org/10.1016/0010-8545(92)80031-L).
- [12]. D.M. Oliveira, P.P. Macaroff, K.F. Ribeiro, Z.G.M. Lacava, R.B. Azevedo, E.C.D. Lima, P.C. Morais, A.C. Tedesco, Studies of zinc phthalocyanine/ magnetic fluid complex as a bifunctional agent for cancer treatment. *J. Magn. Magn. Mater.* 289 (2005) 476-479. <https://doi.org/10.1016/j.jmmm.2004.11.134>.
- [13]. F.L. Primo, M.M.A. Rodrigues, A.R. Simioni, M.V.L.B. Bentley, P.C. Morais, A. Tedesco, In vitro studies of cutaneous retention of magnetic nanoemulsion loaded with zinc phthalocyanine for synergic use in skin cancer treatment. *J. Magn. Magn. Mater.* 320 (14) (2008) 211-214. <https://doi.org/10.1016/j.jmmm.2008.02.050>.
- [14]. M. Kurupparachchi, H. Savoie, A. Lowry, C. Alonso, R.W. Boyle, Polyacrylamide nanoparticles as a delivery dystem in photodynamic therapy. *Mol. Pharmaceut.* 8 (2011) 920-931. <https://doi.org/10.1021/mp200023y>.
- [15]. T.J. Dougherty, C.J. Gomer, B.W. Henderson, G. Jori, D. Kessel, M. Korbelik, J. Moan, Q. Peng, Photodynamic therapy. *J. Natl. Cancer Inst.* 1998 90 889. <https://doi.org/10.1093/jnci/90.12.889>.
- [16]. L.A. Ehrlich, P.J. Skrdla, W.K. Jarrell, J.W. Sibert, N.R. Armstrong, S.S. Saavedra, A.G.M. Barrett, B.M. Hoffman, Preparation of Polyetherol-Appended Sulfur Porphyrines and Investigations of Peripheral Metal Ion Binding in Polar Solvents. *Inorg. Chem.* 39 (2000) 3963-3969. <https://doi.org/10.1021/ic991033m>.
- [17]. S.L.J. Michel, A.G.M. Barrett, B.M. Hoffman, Peripheral Metal-Ion Binding to Tris(thia-oxo crown) Porphyrines. *Inorg. Chem.* 42 (2003) 814. <https://doi.org/10.1021/ic025639d>.
- [18]. M.N. Yarasir, M. Kandaz, B.F. Filiz Şenkal, A. Koca, B. Salih, Metal-ion sensing and agregation studies on reactive phthalocyanines bearing soft-metal receptor moieties; synthesis, spectroscopy and electrochemistry. *Dyes Pigm.* 77 (2008) 7. <https://doi.org/10.1016/j.poly.2007.07.042>.
- [19]. O.A. Tretayakov, F. Erden, Temporal Cavity Oscillations Caused by a Wide-Band Waveform. *Prog. Electromagn. Res. B*, 6 (2008) 183-204. doi:10.2528/PIERB08031222
- [20]. E. Eroğlu, S. Aksoy, O.A. Tretayakov, Surplus of energy for time-domain waveguide modes. *Energy Educ. Sci. Tech.*, 29 (1) (2012) 495-506.
- [21]. M. Celebi, Z.Ö. Özdemir, E. Eroğlu, İ. Güney, Statistically defining optimal conditions of coagulation time of skim milk. *J. Chem. Soc. Pakistan*, 36(1) (2014) 1-5.
- [22]. M. Celebi, Z.Ö. Özdemir, E. Eroglu, M. Altikatoglu, I. Güney Determination of Minimum Enzymatic Decolorization Time of Reactive Dye Solution By Spectroscopic and Mathematical Approach. *Spectrosc. Spect Anal*, 35(2) (2015) 340-345. [https://doi.org/10.3964/j.issn.1000-0593\(2015\)02-0340-06](https://doi.org/10.3964/j.issn.1000-0593(2015)02-0340-06).

- [23]. E. Eroglu, N. Ak, I. Güney, E. Sener, Component analysis of the different fish samples containing heavy metals in Istanbul Bosphorus. *Fresen. Environ. Bull.* 25 (1) (2016) 292-299.
- [24]. J.E. Freund, *Modern Elementary Statistics*, 5th eds. (Prentice Hall, Arizona) 1979.

Bülent Kıyak" The Mathematical Calculations on Absorbance-wavelength Relation of Zinc, Cobalt and Indium Peripherally /Non-Peripherally Metallo Phthalocyanines Bearing Zingerone Moieties" *American Journal of Engineering Research (AJER)*, vol.8, no.02, 2019, pp.260-270